JCI insight

RESEARCH ARTICLE

Autoimmune inner ear disease patient–associated 28-kDa proinflammatory IL-1β fragment results from caspase-7–mediated cleavage in vitro

Shresh Pathak[1,2,3] and Andrea Vambutas[1,2,3,4]

[1]Feinstein Institutes for Medical Research, Manhasset, New York, USA. [2]Department of Otolaryngology, Donald and Barbara Zucker School of Medicine at Hofstra/Northwell, Hempstead, New York, USA. [3]Head and Neck Surgery, Department of Otorhinolaryngology, Montefiore Medical Center, Albert Einstein College of Medicine, Bronx, New York, USA. [4]Department of Molecular Medicine, Donald and Barbara Zucker School of Medicine at Hofstra/Northwell, Hempstead, New York, USA.

Interleukin-1β (IL-1β) is a key proinflammatory cytokine involved in the progression of many autoinflammatory and autoimmune diseases, including autoimmune inner ear disease (AIED). IL-1β inhibition has been shown to result in clinical hearing improvement in a small cohort of corticosteroid-resistant patients with AIED. Canonical processing of pro–IL-1β by caspase-1 generates an active 17-kDa fragment, capable of instigating a proinflammatory microenvironment. However, in response to LPS, PBMCs from patients with AIED uniquely express a 28-kDa IL-1β fragment, as compared with PBMCs from control subjects. We synthesized and compared the biologic activity of the 28-kDa fragment to the 17-kDa IL-1β product and the pro–IL-1 31-kDa protein. The 28-kDa IL-1β fragment induces IL-6, TNF-α, and CCL3 in PBMCs. Uniquely, only caspase-7 treatment showed a dose- and time-dependent increase in 28-kDa band generation. Mass spectrometry confirmed the putative caspase-7 cleavage site of pro–IL-1β, which was used to generate the 28-kDa fragment used for PBMC stimulation studies. Collectively, these results provide insight into the function of a poorly understood, processed 28-kDa form of IL-1β in patients with AIED that is uniquely generated by caspase-7 and is capable of activating further downstream proinflammatory cytokines. Further investigation may provide novel pharmacologic targets for the treatment of this rare disease.

Introduction

Autoimmune inner ear disease (AIED) is a rare, yet-to-be-classified orphan disease (1) characterized by periods of acute hearing decline triggered by unknown stimuli (2). Affected patients do not have affected first-degree relatives, arguing against a monogenic disease. Treatment consists of corticosteroids, which are initially effective in 70% of patients; however, the responsiveness dramatically declines over time (14% remain responsive at 3 years) (3). Unfortunately, for those patients who do not respond to corticosteroids, alternative immunosuppressive agents have not been efficacious (4, 5). Understanding the biologic mechanisms underpinning this disease has been further complicated by a lack of a robust animal model that can recapitulate human disease. Although an elegant cochlin peptide–vaccinated model was shown in 2004 (6), further studies using this model have not been published. Similarly, a keyhole limpet hemocyanin–challenged guinea pig model has been used; however, whereas TNF inhibition was effective in this model (7), it was ineffective in human patients with AIED (5, 8). We initially studied human patients with AIED undergoing cochlear implantation by evaluating their PBMCs stimulated with autologous cochlear perilymph to gain insight as to the potential inflammatory pathways in this disease. As a result, we identified differential expression of the IL-1 decoy receptor (IL1R2) (9), and subsequently, overexpression of IL-1β in patients with corticosteroid-resistant AIED (10). IL-1β is a proinflammatory cytokine that is instrumental in the development of inflammation and the exacerbation of many autoimmune and autoinflammatory diseases. IL-1β plays a homeostatic role in daily biologic processes, but its constitutive overproduction is associated with chronic diseases such as type 1

Conflict of interest: The authors have declared that no conflict of interest exists.

Submitted: June 4, 2019
Accepted: December 26, 2019
Published: February 13, 2020.

Reference information: *JCI Insight*. 2020;5(3):e130845. https://doi.org/10.1172/jci.insight.130845.

diabetes (11), rheumatoid arthritis (12, 13), osteoarthritis, inflammatory bowel disease (14), multiple sclerosis (15), Muckle-Wells syndrome (16, 17), and corticosteroid-resistant AIED (10). IL-1β is processed by a series of proteins, which collectively are referred to as the inflammasome. Genetic mutations occurring in the different components of the inflammasome and resultant overproduction of IL-1β (18, 19) are clinically manifest in many autoinflammatory diseases, such as familial cold autoinflammatory syndrome, Muckle-Wells syndrome, and chronic infantile neurologic cutaneous articular syndrome (18, 20–22). We have previously demonstrated that IL-1β inhibition was effective in a small cohort of corticosteroid-resistant patients with AIED, where reduction of IL-1β plasma levels was associated with clinical hearing improvement (23). IL-1β is produced by a variety of cell types, including monocytes, macrophages, dendritic cells, B lymphocytes, and NK cells (24–26). IL-1β is a master regulator cytokine and thereby influences a number of downstream molecules. IL-1β induces matrix metalloproteinase-9 (MMP-9) (27–29), which is also overexpressed in corticosteroid-resistant patients with AIED (10). MMP-9, in turn, is involved in downstream inflammatory processes and has been shown to increase the permeability of the blood-brain barrier (30) and therefore may exert a similar effect on the blood-labyrinthine barrier. MMP-9's counterbalancing molecule, tissue inhibitor of metalloproteinase-1 (TIMP-1), is also induced by IL-1β (31). Corticosteroid-responsive patients have higher basal TIMP-1 levels, and their PBMCs express more TIMP-1 in response to IL-1β, which may afford them greater protection and resultant hearing preservation than corticosteroid-resistant patients with AIED (32). IL-1β has been shown to induce chemokine (CC motif) ligand 3 (CCL3) (also known as macrophage inflammatory protein 1-α), which is upregulated in type 1 diabetes mellitus and other autoimmune diseases (33, 34). Various mechanisms of IL-1β processing have been proposed, the most widely accepted of which is through the action of the protease caspase-1/IL-1 converting enzyme (ICE) (35). IL-1β is produced as a 31-kDa propeptide (36) and is converted into active 17-kDa form by caspase-1 (35). Caspase-1's mode of action was first reported in 1989 (37, 38), and its specificity for IL-1β was confirmed by Sleath et al. in 1990 (39). Caspase-1–deficient mice lack the ability to release active IL-1β (40). The 269–amino acid IL-1β precursor (pro–IL-1β) (molecular weight 31 kDa) is cleaved to generate a 153–amino acid, mature segment between Asp^{116} and Ala^{117} (41–44), which is the most well recognized product of ICE cleavage and results in production of mature 17 kDa, a stretch of residues extending from 117 to 269 (37, 38). ICE cleavage occurs at more than 1 site in IL-1β: a second cleavage site between Asp^{27} and Gly^{28} generates a 28-kDa fragment (residues 28 through 269) (45). Puren et al., in 1999, reported generation of a 28-kDa fragment as an early cleavage form of pro–IL-1β by LPS-stimulated PBMCs (46). Moreover, in addition to caspase-1, generation of the 28-kDa fragment was reported to be mediated by caspase-8 (47), MMP-3, and MMP-9 (48). Little is known about the biologic activity of the 28-kDa fragment. In one study, it was identified to have antiinflammatory properties by interfering with mature IL-1β signaling (49). In the present study, we have characterized the biologic activity of the 28-kDa fragment of IL-1β because the majority of PBMCs from patients with AIED uniquely and strongly express the 28-kDa product in response to in vitro LPS stimulation and only a few patients express the canonical 17-kDa product of IL-1β compared with disease-free, healthy control patients. Clinically we have previously observed that in an open-label, early-phase clinical trial, corticosteroid-resistant patients with AIED benefited from IL-1β inhibition, where hearing improvement correlated with a reduction in circulating IL-1β (23), which thereby suggested that IL-1β was biologically active and pathogenic in these patients.

Results

In the present study, we have identified that the 28-kDa fragment of IL-1β is expressed in PBMCs from patients with AIED in response to LPS, and this fragment is capable of inducing other downstream proinflammatory cytokines. We have further determined that the 28-kDa fragment is uniquely generated by caspase-7 cleavage of pro–IL-1β.

LPS-stimulated PBMCs of patients with AIED exhibit preferential processing of IL-1β to generate a 28-kDa fragment. When cultured PBMCs were stimulated with LPS and protein fragments separated by molecular weight using Western blot analysis, we observed that the 28-kDa fragment generated during LPS-induced IL-1β processing is unique to patients with AIED (n = 30) when compared with normal healthy subjects (n = 24), because normal healthy subjects did not express the band or had minimal expression of this band (Figure 1A). The anticipated IL-1β 17-kDa fragment was not present in AIED patient samples. Presence of the 28-kDa band did not correlate with increased caspase-1 expression (Figure 1A); however, a mild enhancement of caspase-7 expression was observed in patients with AIED having an LPS-induced 28-kDa fragment of IL-1β when compared with control subjects. The intensity of the 28-kDa band

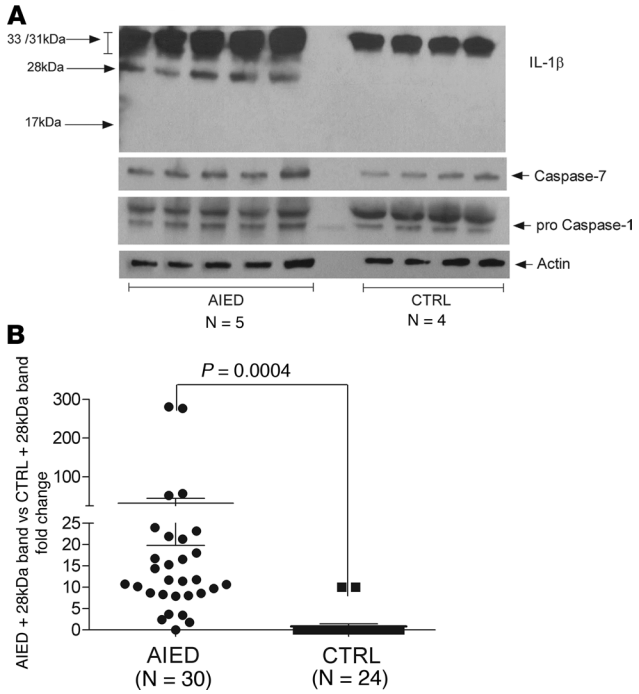

Figure 1. PBMCs from patients with AIED uniquely express a 28-kDa fragment in response to LPS. (**A**) Western blot analysis of PBMCs of several representative patients with AIED (n = 5 out of 30 patients with AIED with 28-kDa band observed) and control subjects (n = 4 out of 24 control subjects studied). PBMCs were treated with 1 μg/mL LPS, and processing of IL-1β was determined by Western blot using anti–IL-1β antibody (it identifies a proform doublet at 33/31 kDa and bands at 28 kDa and 17 kDa, R&D Systems). These representative samples demonstrate generation of a 28-kDa IL-1β band in LPS-stimulated PBMCs from patients with AIED. Generation of the 28-kDa IL-1β is not the result of variability in the amount of detectable caspase-7 (34 kDa) or pro–caspase-1 (a doublet of 50/48 kDa). The majority of samples were analyzed twice; however, in several instances the AIED patient samples were exhausted (>66% run in duplicate). (**B**) Relative quantification of the 28-kDa band, as normalized to actin in both groups, by densitometry analysis software ImageJ (NIH) revealed statistically significant differences analyzed by Mann-Whitney U test (P = 0.0004) between patients with AIED (n = 30) and control subjects (n = 24).

(normalized against actin) was 27-fold higher in patients with AIED compared with control subjects (Figure 1B). This difference was statistically significant when compared by Mann-Whitney U test (P = 0.0004). Based on previously reported caspase-1 cleavage sites (45), we synthesized full-length 31-kDa, 28-kDa, and 17-kDa IL-1β fragments to investigate the biologic activity of each fragment (Figure 2). We confirmed that these synthetic fragments had no endogenous endotoxin prior to use.

The 28-kDa fragment of IL-1β mildly induces IL-1β, IL-6, and CCL3 mRNA expression. PBMCs from patients with AIED and control subjects were stimulated with pro–IL-1β (31-kDa fragment), the 17-kDa fragment, and the 28-kDa IL-1β fragment and compared with LPS or recombinant active 17-kDa IL-1β (Peprotech) and compared for RNA expression of several cytokines downstream of IL-1β. PBMCs of control subjects treated with the 28-kDa IL-1β fragment had mildly increased expression of IL-1β, IL-6, and CCL3 mRNA (Figure 3), although this did not result in statistical significance. The induction was greater than in PBMCs from patients with AIED, possibly suggesting some degree of endogenous T cell polarization in the AIED PBMCs. In patients with AIED, the 17-kDa and 28-kDa fragments were equally effective in inducing IL-1β and IL-6 mRNA expression. Statistical significance was achieved for the difference in expression for IL-1β in response to the 28-kDa and 17-kDa fragments in control subjects (P = 0.016). The 17-kDa fragment was less effective than the 28-kDa fragment in inducing TIMP-1 in controls but not patients with AIED. This would imply that in healthy patients, counter-regulatory mechanisms are in place to reduce inflammation. MMP-9 and TIMP-1 expression was greater with both the 28-kDa and 17-kDa fragments of IL-1β than with LPS (Figure 3). To determine whether any counterbalancing Th2 cytokines were induced, we assessed IL-10, IL-13, and TGF-β mRNA expression in PBMCs from patients and controls as well. We performed qPCR for IL-10, IL-13, and TGF-β for a subset of PBMCs from patients and controls. In both patients and controls, no induction was observed

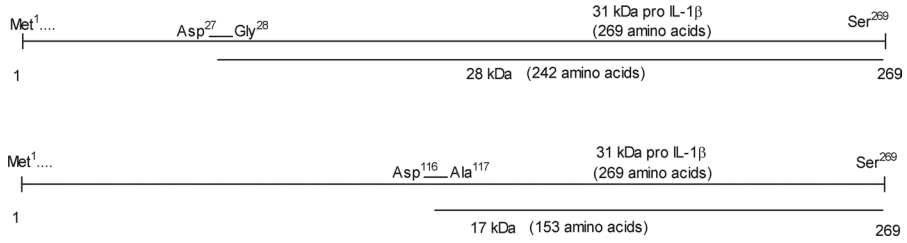

Figure 2. Map of IL-1β fragments and expression of the 28-kDa fragment of IL-1β in AIED subjects. Map of IL-1β fragments depicting size of the fragments and position of cleavage sites, which result in generation of 28 kDa and 17 kDa.

with the 3 IL-1β fragments. In the case of IL-10, increased expression was observed in response to LPS but not to the 3 fragments. In the case of IL-13, minimal to no expression could be detected in all experimental conditions. In the case of TGF-β, robust expression was observed in untreated patients and controls, and it was not further augmented with either LPS or the 3 IL-1β fragments (data not shown).

The 28-kDa fragment of IL-1β induces CCL3, TNF-α, and MMP-9 release. We also examined release of CCL3, TNF-α, MMP-9, IL-6, TIMP-1, and IL-4 into the culture supernatants following treatment of PBMCs with the 28-kDa and 17-kDa IL-1β fragments as compared with LPS (positive control), rIL-1β (17 kDa, Peprotech), and full-length 31-kDa pro–IL-1β (negative control). The 28-kDa fragment induced CCL3 release more than the 17-kDa fragment in patients with AIED (n = 10) and controls (n = 8); although a trend was observed, statistical significance was not reached (P = 0.027 for the control group, Figure 4A). As with CCL3, the 28-kDa fragment of IL-1β induced TNF-α release more effectively than the 17-kDa fragment in PBMCs from both patients and controls (patients with AIED, n = 10, and control subjects, n = 8); statistical significance was achieved for the control group only (P = 0.008, Figure 4B). As expected, the 31-kDa fragment again had no effect (Figure 4B). An IL-6 ELISA was performed on conditioned supernatant samples from PBMCs of patients with AIED (n = 9) and control subjects (n = 9) stimulated with either various IL-1β fragments or LPS (Figure 4A). Minimal increases in response to the 28-kDa IL-1β fragment as compared with the 17-kDa fragment were observed but were not significant (Figure 4C).

MMP-9 release was similarly assessed in conditioned supernatant of PBMCs of patients with AIED (n = 11) and control subjects (n = 9) treated with the same IL-1β fragments. MMP-9 was induced close to 3-fold by the 28-kDa fragment in patients with AIED whereas there was no observed induction in PBMCs from control subjects. A trend was observed in control PBMCs in response to the 28-kDa fragment as compared with the 17-kDa fragment (P = 0.027).

Because of our previous observations that the balance of MMP-9 to TIMP-1 had clinical importance (32) and that MMP-9 was preferentially induced by the 28-kDa fragment, we interrogated whether a similar effect on TIMP-1 was observed. The 28-kDa fragment of IL-1β was not able to induce TIMP-1 as compared with the 31-kDa or untreated PBMCs in both groups (PBMCs from patients with AIED, n = 11, and control subjects, n = 9) (Figure 4E).

Finally, an IL-4 ELISA was done to determine whether the 28-kDa fragment has antiinflammatory properties as previously reported in another system (49). Conditioned supernatant from treated PBMCs with all 3 fragments of IL-1β along with LPS from patients with AIED (n = 11) and control subjects (n = 8) was compared to untreated samples and evaluated by ELISA (Figure 4F). All IL-1β fragments, including the 28-kDa fragment, failed to induce IL-4 release, demonstrating the expected antiinflammatory IL-4 was not a counterbalancing cytokine in our patient cohort.

The 28-kDa band of IL-1β can be generated by caspase-7–mediated cleavage. To identify which caspase was involved in generation of the 28-kDa fragment of IL-1β, recombinant pro–IL-1β was incubated with caspase-1 to -10, separated by SDS gel electrophoresis, and subjected to Western blot. Only caspase-7 demonstrated generation of the 28-kDa fragment (Figure 5, A and B). Caspase-1–mediated cleavage resulted in generation of 17 kDa (Figure 5A), whereas caspase-7–mediated cleavage of pro–IL-1β resulted in generation of 28 kDa (Figure 5B). Caspase-7 showed a dose-dependent and time-dependent increase in 28-kDa band generation, indicating that caspase-7 could generate the 28-kDa band of IL-1β (Figure 6).

Caspase-3/7 inhibitor CAY 10406 inhibits caspase-7 and the 28-kDa fragment of IL-1β in a dose-dependent manner. We next studied whether specific inhibition of caspase-7 could affect the processing of the 28-kDa band of

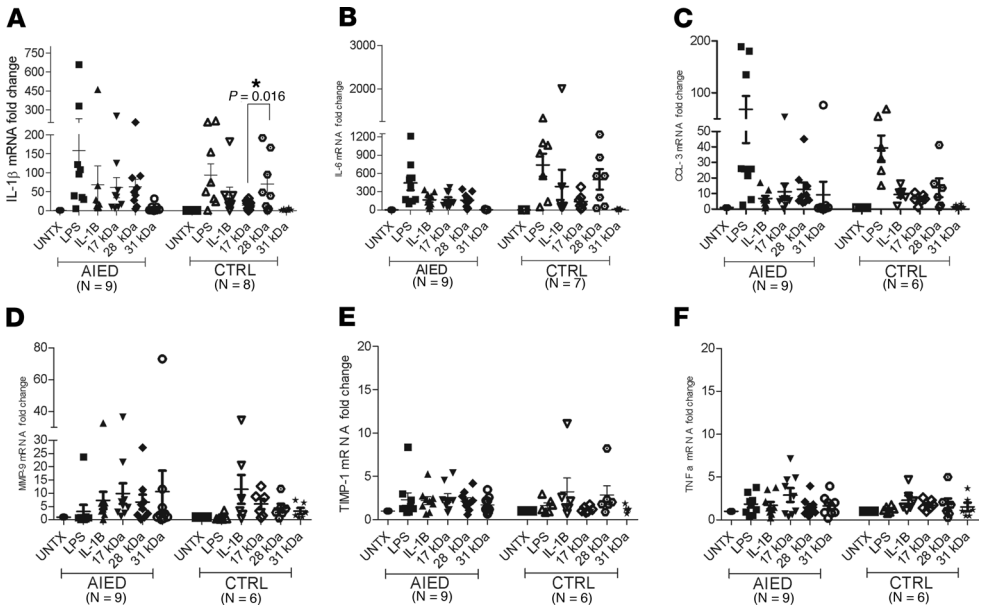

Figure 3. The 28-kDa fragment of IL-1β induces greater proinflammatory cytokine mRNA expression than the canonical 17-kDa fragment and greater TIMP-1 expression in control PBMCs. Expression levels of (**A**) IL-1β, (**B**) IL-6, (**C**) CCL3, (**D**) MMP-9, (**E**) TIMP-1, and (**F**) TNF-α mRNA from PBMCs of patients with AIED (*n* = 9) and controls (*n* is shown for each panel) treated with 1 μg/mL LPS (positive control); recombinant IL-1β (rIL-1β) (Peprotech); or 17-kDa, 28-kDa, and 31-kDa (negative control) fragments of IL-1β or left untreated. The expression levels were measured in replicate samples by real-time quantitative PCR (qPCR) using 480 LightCycler. Data shown are mean ± SEM. The threshold cycle (Ct) value was calculated from amplification plots, and gene expression was normalized using the Ct of the housekeeping gene glyceraldehyde-3-phosphate. Fold induction of the target gene was calculated using the formula $2^{-\Delta\Delta Ct}$. Statistical significance was achieved for the difference in expression for IL-1β in response to the 28-kDa and 17-kDa fragments in control subjects ($P = 0.016$). Although differences were observed between expression in response to the 28-kDa and 17-kDa fragments for IL-6 and CCL3, these did not achieve significance. MMP-9 and TNF-α expression showed minimal, insignificant changes in response to the IL-1 fragments. The Wilcoxon signed-rank test was performed for paired observations, to compare expression levels within groups, in response to the 17-kDa and 28-kDa fragments. For the pairwise comparison of 17-kDa and 28-kDa fragments, a Bonferroni's adjustment was made for the 2 hypothesis tests carried out within a cytokine. The 2 tests were carried out comparing 17-kDa and 28-kDa fragments within the AIED group and within the control group, such that any given comparison required $P < (0.05 / 2) = 0.025$. Each experiment was repeated twice to confirm reproducibility.

IL-1β. LPS-stimulated PBMCs were treated with different concentrations of the caspase-3/7 inhibitor, CAY 10406. Inhibition of caspase-7 was observed in a dose-dependent manner, which was accompanied by a dose-dependent inhibition of 28-kDa band formation (Figure 7). Cell viability was between 70% and 85% in all treated samples; therefore, inhibition was not a result of toxicity associated with the use of the inhibitor. This experiment demonstrates that caspase-7 is involved in the generation of the 28-kDa fragment of IL-1β.

The 28-kDa fragment of IL-1β is preferentially secreted from PBMCs of patients with AIED. Supernatants from LPS-treated PBMCs of patients with AIED (*n* = 13) and control subjects (*n* = 14) were separated by SDS-PAGE followed by Western blot. Conditioned medium of PBMCs from the patients with AIED (13 out of 13 patients) showed a strong 28-kDa band, and 4 of 13 showed a faint 17-kDa band; controls showed 5 faint 28-kDa bands out of a total of 14 controls (Figure 8).

LPS-stimulated THP-1 cells generate the 28-kDa fragment of IL-1β. We subsequently investigated whether the human monocytic cell line THP-1 (ATCC, TIB-202) demonstrated similar processing of IL-1β as observed in patients with AIED. IL-1β expression was measured by Western blot analysis for the 28-kDa IL-1β fragment generation. As anticipated (based on prior publications from other groups) (50), the 28-kDa fragment could be identified in THP-1 cells (Figure 9), which thus provides a consistent source of cells for further mechanistic studies. Because of a background issue, direct immunoprecipitation was done to get a relatively clean band.

Confirmation of putative caspase-7 cleavage site of pro–IL-1. Generation of the 28-kDa IL-1β fragment was based on an anticipated caspase-1 cleavage site, not an unanticipated caspase-7 cleavage. For this reason, we sought to confirm the site of cleavage of pro–IL-1β to be Asp^{27} to Gly^{28}. Purified pro–IL-1β was digested with caspase-7 and the 28-kDa band was excised. The resulting peptide was subjected to analysis by

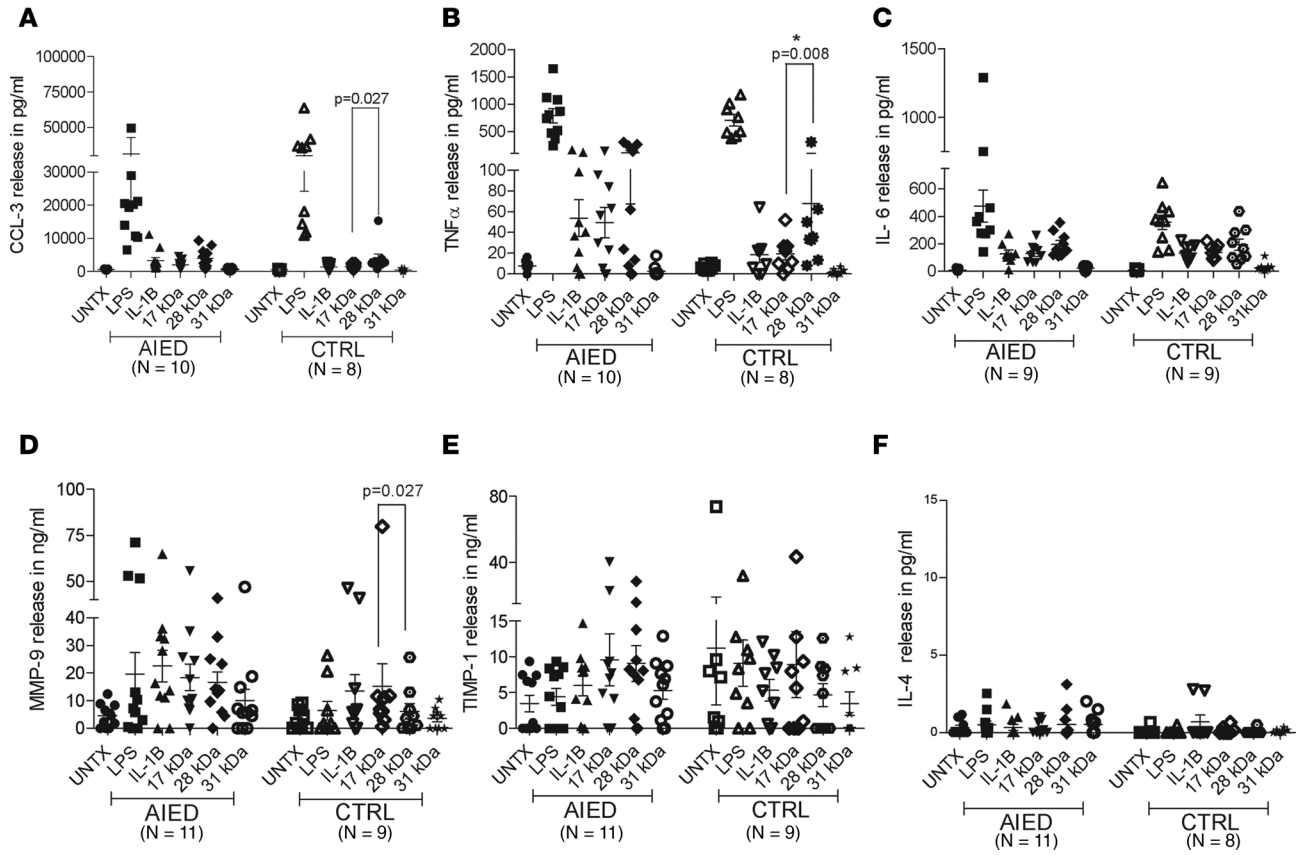

Figure 4. The 28-kDa fragment of IL-1β induces release of CCL3, TNF-α, and MMP-9. PBMCs of patients with AIED and controls (*n* is shown for each panel) were treated with 1 μg/mL LPS (positive control); rIL-1β; or 17-kDa, 28-kDa, and 31-kDa (negative control) fragments of IL-1β or left untreated (16 hours). Cytokines were measured by ELISA from the culture supernatants. Data represent the mean ± SEM in all panels. (**A**) The concentration of CCL3 was measured by ELISA from the culture supernatants. A trend was observed in control PBMCs in response to the 28-kDa fragment as compared with the 17-kDa fragment ($P = 0.027$). (**B**) The TNF-α concentration was determined using a TNF-α ELISA kit. A statistically significant difference was observed in control PBMCs in response to the 28-kDa fragment as compared with the 17-kDa fragment ($P = 0.008$). (**C**) IL-6 concentrations in culture supernatants were determined by ELISA. (**D**) MMP-9 levels were detected by ELISA in the culture supernatant. A trend was observed in control PBMCs in response to the 28-kDa fragment as compared with the 17-kDa fragment ($P = 0.027$). (**E**) TIMP-1 supernatant concentrations were similarly measured by ELISA. (**F**) To determine whether the 28-kDa fragment of IL-1β had antiinflammatory properties, PBMCs of AIED and control subjects were assayed for IL-4 release by ELISA. For **A**–**F**, the Wilcoxon signed-rank test was performed for paired observations, to compare expression levels within groups, between 17 kDa and 28 kDa. For the pairwise comparison of 17 kDa and 28 kDa, a Bonferroni's adjustment was made for the 2 hypothesis tests carried out within a cytokine. The 2 tests were carried out comparing 17 kDa and 28 kDa within the AIED group and within the control group, such that any given comparison required $P < (0.05 / 2) = 0.025$. Each experiment was repeated twice to confirm reproducibility.

mass spectrometry, and data were processed by MaxQuant computational platform. Mass spectrometry data were searched against UniProt human sequence. The identified stretches of IL-1β are highlighted in red (Figure 10). Because of the low sequence coverage, it was difficult to locate the exact N-terminus; however, the identified peptide stretch CSFQDLDLCPLDGGIQLR is immediately downstream of the predicted putative 28-kDa cleavage site GPKQMKCSFQDLDLCPLDGGIQLR, with a difference in the first 6 amino acids (Figure 10). Therefore, Asp^{27} to Gly^{28} is the likely site of cleavage with caspase-7 because all caspases require an aspartic acid residue for cleavage.

Discussion

In the present study, we report that PBMCs of patients with AIED ($n = 30$) expressed a 28-kDa fragment of IL-1β when treated with LPS, which was either absent or minimally expressed in control subjects ($n = 24$) (Figure 1). Moreover, this 28-kDa fragment, generated by N-terminal cleavage of pro–IL-1β, appears to have proinflammatory biologic activity, as evidenced by the induction of IL-1β, IL-6, and CCL3 mRNA expression (Figure 3), as well as CCL3 and TNF-α release from PBMCs from patients with AIED as well as controls (Figure 4). Additionally, the 28-kDa fragment induced release of MMP-9 in patients with AIED preferentially over controls (Figure 4). Intriguingly, we observed the 28-kDa

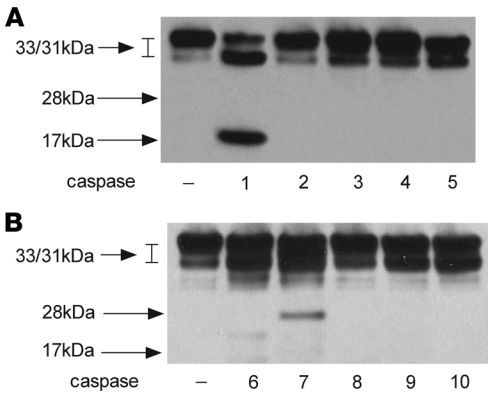

Figure 5. Caspase-7 uniquely cleaves pro–IL-1β to generate the 28-kDa fragment. Western blot was performed on caspase-1– through -10–treated (1 unit for each caspase) recombinant pro–IL-1β (200 ng, incubated for 2 hours at 37°C). The resulting cleavage products were separated on a 12% gel and then analyzed by Western blotting using anti–IL-1β mouse monoclonal antibody at 1:500 dilution. Experiments were repeated 3 times to confirm reproducibility. (**A**) Caspase-1 through -5. (**B**) Caspase-6 through -10.

fragment induced TIMP-1 mRNA expression (Figure 3), in controls preferentially over patients, and therefore may further prevent these patients with AIED from regulating inflammation, although release of TIMP-1 was highly variable in both patients and controls. Interestingly, the 28-kDa fragment resulted in greater induction of proinflammatory cytokines in control PBMCs as compared with PBMCs from patients with AIED. We hypothesize that these observations are a result of higher endogenous basal levels of inflammation in PBMCs of patients with AIED. Patient PBMCs, therefore, may be less capable of responding to weaker inflammatory stimuli, whereas they still can mount a strong response to LPS. Similarly, specific N-terminal cleavage of other IL-1 family members has resulted in a strong induction of proinflammatory activity: in IL-36, specific N-terminus cleavage resulted in very significant increases (in excess of 10^3-fold) in activity and receptor binding (51). This N-terminal IL-36 cleavage is mediated by caspase-3 (52). A previous report showed the 28-kDa band of IL-1β had antiinflammatory properties; in our patients with AIED, no IL-4 was generated (Figure 4F), and TIMP-1 release was not specifically affected. Consistent with our observations, others have shown that processing of IL-1β into the 28-kDa form upon statin stimulation is not abrogated with either caspase-1– or ASC-knockout macrophages (49). However, as expected, these knockouts did completely abrogate generation of the 17-kDa mature IL-1β, suggesting the potential role of other caspases in the generation of the 28-kDa fragment. For this reason, we investigated the ability of other caspases (caspase-2 to caspase-10) to generate a 28-kDa IL-1β fragment. Our results indicated that only caspase-7 seems to be involved in processing pro–IL-1β to generate the 28-kDa fragment (Figures 5–7). This was further supported by using the caspase-3/7 inhibitor (CAY 10406), which was able to decrease caspase-7 levels and generation of the 28-kDa fragment of IL-1β in a dose-dependent manner. Specific caspase-7 inhibitors are not readily available because caspase-7 has functional and structural similarities with caspase-3 (53). There could be an argument that CAY 10406 is a common inhibitor for both caspases, but in our experiments we did not see any digestion of pro–IL-1β by caspase-3 (Figure 5), implying that the 28-kDa IL-1β fragment generation was due to caspase-7. It has been shown that in peritoneal macrophages of caspase-7–knockout mice, caspase-1 mediates caspase-7 activation when stimulated with LPS (54), indicating there are common

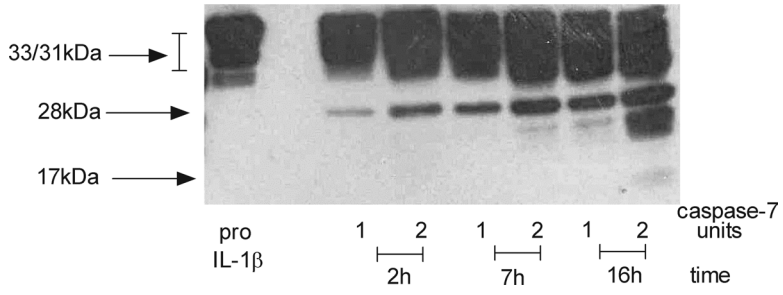

Figure 6. Caspase-7 generates the 28-kDa IL-1β fragment in a dose- and time-dependent manner. Western blot done on samples containing recombinant pro–IL-1β (200 ng) incubated with caspase-7 (1 unit or 2 units) for 2 hours, 7 hours, and 16 hours at 37°C. The resulting cleavage products were separated on a 12% gel and analyzed by Western blotting using anti–IL-1β mouse monoclonal antibody at 1:500 dilution. Experiments were repeated twice to confirm the reproducibility.

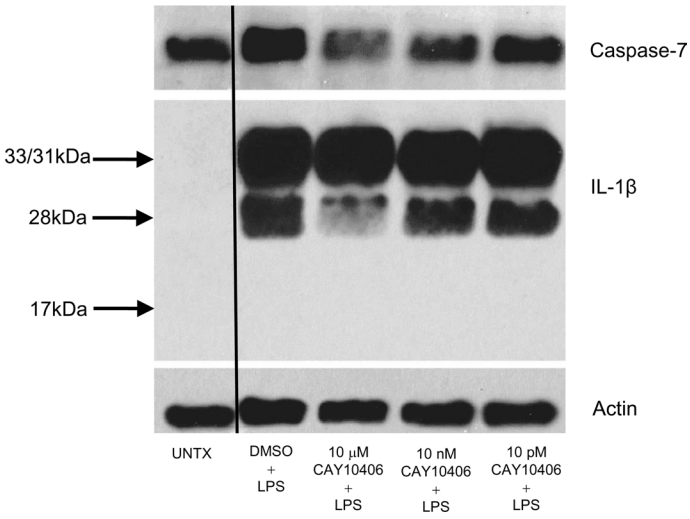

Figure 7. Caspase-7 inhibition results in loss of the 28-kDa IL-1β fragment. PBMCs of control subjects were treated with 1 μg/mL LPS with DMSO or LPS in combination with CAY 10406 (caspase-3/7 inhibitor) at concentrations of 10 μM, 10 nM, and 10 pM along with no treatment. The samples were subjected to Western blotting using caspase-7 antibody and IL-1β antibody. β-Actin was used as an internal control for immunoblotting. A thin black line indicates noncontiguous lanes from the same gel.

pathways connecting inflammatory and apoptotic caspases. Although caspase-7 and caspase-3 exhibit many functional similarities, they show different activity for natural substrates (53). This may explain our observations that caspase-7 was able to cleave pro–IL-1β, whereas caspase-3 could not. Further support of these differences is garnered from a recent report where splenocytes of mice exposed to LPS developed activation of caspase-7, whereas caspase-7–deficient mice were refractory to LPS-induced lymphocyte apoptosis (55). Cleaved caspase-7 has clearly been demonstrated in the cochlea in response to ototoxic stimuli (56). Moreover, caspase-7 has been shown to be involved in activation of microglia (57), resident cells in both the cochlea and the brain (58–60). Our experiments demonstrate that patients with AIED exhibited novel processing of IL-1β in response to LPS by caspase-7. Furthermore, the 28-kDa fragment of IL-1β resulted in induction and release of other proinflammatory cytokines, greater than or comparable to the mature canonical 17-kDa fragment of IL-1β. The 28-kDa fragment of IL-1β was detected in the supernatants of all patients with AIED (13 out 13 patients) compared with control subjects, where supernatants of only 5 out of 14 showed a faint 28-kDa band when immunoblotted with IL-1β (Figure 8). This observation suggests that patients with AIED demonstrate a unique method of processing IL-1β that results in a strongly proinflammatory microenvironment. Interestingly, in some culture supernatants, both the 28-kDa and the 17-kDa bands are observed, whereas intracellularly, the 28-kDa band is preferentially observed in response to LPS. It is possible that the 28-kDa IL-1β fragment is further processed into the 17-kDa product. Experiments are underway to identify the intracellular localization and stability of the 28-kDa product. We initially generated the 28-kDa protein based on a putative caspase-1 cleavage site and did not anticipate caspase-7 to generate this fragment. To confirm the site of pro–IL-1 β cleavage by caspase-7 for generation of the 28-kDa band, pro–IL-1β was

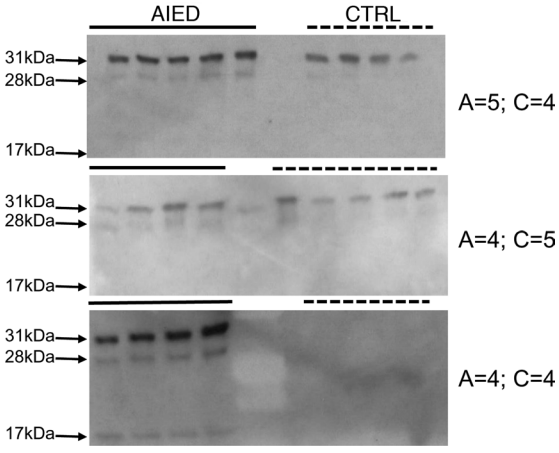

Figure 8. The 28-kDa fragment of IL-1β can be detected in cultured supernatants. PBMCs of patients with AIED (n = 13) and control subjects (n = 14) were treated with 1 μg/mL LPS for 16 hours; conditioned medium was then analyzed by Western blot using IL-1β antibody at 1:250 dilution. The 28-kDa band was observed in 13 of 13 patients with AIED, and a weak 28-kDa band was observed in 4 out of 14 controls. This experiment was run 3 times; however, not all samples were available for all 3 experiments.

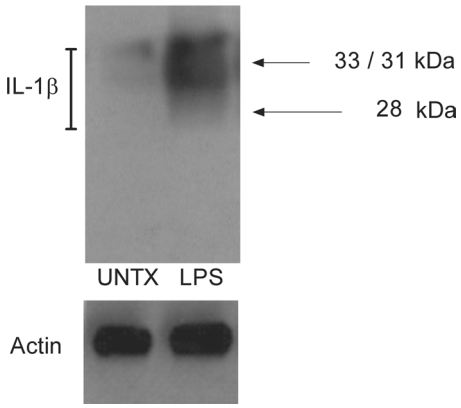

Figure 9. The 28-kDa IL-1β band is observed in LPS-stimulated THP-1 cells. The 28-kDa fragment of IL-1β was detected in THP-1. THP-1 cells were treated with LPS (1 μg/mL) for 16 hours, then analyzed by Western blot using IL-1β antibody at 1:250 dilution. β-Actin was used as an internal control for immunoblotting. Experiments were repeated twice to confirm the reproducibility.

exposed to caspase-7 and separated by SDS-PAGE, excised, and analyzed by mass spectrometry. Mass spectrometry data indicated that the identified peptide stretch CSFQDLDLCPLDGGIQLR is 6 amino acids away from the putative 28-kDa band cleavage site GPKQMKCSFQDLDLCPLDGGIQLR (Figure 10). Total identified peptide stretch by mass spectrometry covered about 26% of the total 28-kDa sequence. Given the absolute requirement for caspases to cleave after an aspartic acid residue (61), there is little doubt that caspase-7 acted at Asp^{27} to Gly^{28}. In our previous open-label trial of IL-1β blockade in corticosteroid-resistant patients with AIED, we observed hearing improvement, which correlated with reduction of plasma IL-1β (23). Considering the above data, a greater understanding of the mechanism of caspase-7 generation of the IL-1β 28-kDa fragment in these patients may elucidate new pharmacologic targets for disease intervention. Further investigation could yield valuable insights into the post-translational regulation of IL-1β and possible pathophysiology of patients with AIED.

Methods

Preparation of human PBMCs. Human PBMCs were isolated from buffy coats of heparinized blood from healthy donors and patients with AIED using gradient density centrifugation as described previously (10). Cell pellets were washed twice with RPMI 1640 (Thermo Fisher Scientific), counted using a Z2 Coulter Particle Count and Size Analyzer (Beckman Coulter Life Sciences), and then plated in 24-well plate (Costar) at 1×10^6/mL, in RPMI (Thermo Fisher Scientific) containing 10% decomplemented fetal bovine serum (Atlanta Biologicals) 100 U/mL penicillin (Thermo Fisher Scientific) and 100 μg/mL streptomycin (Thermo Fisher Scientific) at 37°C in a 5% CO_2 saturated humidity incubator. After 16 hours of incubation the supernatant was removed. On average, PBMCs' viability, tested using Cellometer (Nexcelom Bioscience), exceeded 80% with a 1:1 ratio of cultured cells and 0.4% trypan blue solution (Thermo Fisher Scientific).

Cell lines used. Human monocytic cell line THP-1 (TIB-202) was purchased from ATCC. Cells were cultured in RPMI 1640 (Life Technologies) and supplemented with 10% fetal bovine serum (Atlanta Biologicals), 4.1 mM L-glutamine, 100 U/mL penicillin, and 100 mg/mL streptomycin (Life Technologies) maintained at 5% CO_2, 37°C.

Protein expression of pro–IL-1β and other fragments of IL-1β and endotoxin assessment. Protein expression in *E. coli* (full-length 31-kDa form of IL-1β, 28-kDa fragment of IL-1β, and 17-kDa mature form of IL-1β) is shown in Supplemental Table 1 (supplemental material available online with this article; https://doi.org/10.1172/jci.insight.130845DS1). These forms were synthesized by LifeTein, LLC, as cDNA expression constructs using the sequences provided in Figure 2, under a T7 promoter, with a glutathione-*S*-transferase (GST) tag and tobacco etch virus (TEV) protease recognition site, and were grown in *E. coli*, with cells lysed and separated by GST affinity chromatography, followed by on-resin cleavage with TEV protease, gel filtration, and endotoxin removal (LifeTein, LLC). Upon arrival in our laboratory, endotoxin levels of custom-made IL-1β subunits from LifeTein, LLC, were measured in our lab to verify they were endotoxin free using limulus amebocyte lysate (LAL) assay for endotoxin content (Pierce LAL chromogenic endotoxin quantitation kit, Thermo Fisher Scientific, 88282).

We also utilized a commercial 17-kDa rIL-1β (Peprotech) in all experiments as a comparator for our synthetic 17-kDa fragment. To validate the bioactivity of the IL-1β fragments, PBMCs of patients with AIED and healthy controls were treated at the same molar concentration (1.18 nM) of all 3 IL-1β

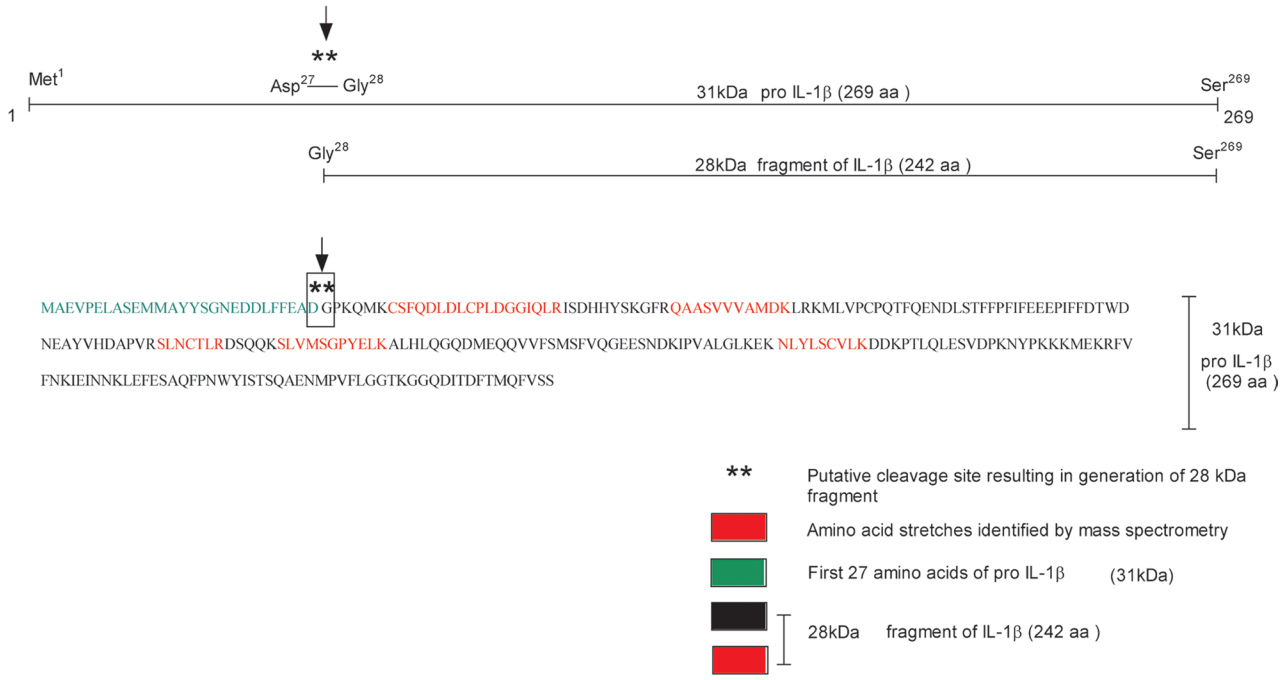

Figure 10. Mapping of putative caspase-7 cleavage site by mass spectrometry. Pro–IL-1β was digested with caspase-7 and the protein fragments separated by 12% SDS-PAGE and identified by silver stain. The resulting 28-kDa peptide was subjected to analysis by mass spectrometry, and data were processed by MaxQuant computational platform. Mass spectrometry data were searched against UniProt human sequence. The identified amino acid stretches of IL-1β are highlighted in red.

fragments overnight and compared with LPS and commercially available 17-kDa IL-1β for their effect on RNA and protein expression as measured by real-time PCR and ELISA.

RNA isolation and quantitative real-time PCR. RNA was isolated from PBMCs using RNeasy Mini Kit (Qiagen) as per the supplier's instructions. The qPCR was performed in a Roche LightCycler 480 as previously described (10). Each reaction contained 16 ng of RNA, 4 μM forward/reverse primer mix, 1 μM probe from the Roche Universal Probe Library (UPL; Roche Applied Science), and Eurogentec qRT-PCR Mastermix (Eurogentec). The PCR primers and UPL probes used are presented in Supplemental Table 2. For each experiment at least 2 replicates were used for analysis.

Western blotting for IL-1β, caspase-1, and caspase-7. Twenty micrograms of proteins, unless otherwise indicated, were fractionated by SDS-PAGE (using 12% or 4%–15% gradient gel) and transferred to a PVDF membrane (all from Bio-Rad) overnight at 45 mA (all steps except primary antibody incubation were carried out at room temperature, with gentle shaking). After 60 minutes in blocking buffer (5% nonfat dry milk [NFDM] from Bio-Rad in 0.05% TBS–Tween-20 [TBST] from Thermo Fisher Scientific), membranes were incubated overnight either with mouse anti–human IL-1β monoclonal antibody (MAB201, R&D Systems), at a concentration of 1:500, or with 1:1000 caspase-1 (sc-515) caspase-1 p10 antibody (C-20) (Santa Cruz Biotechnology) at a concentration of 1:200 and caspase-7 at 1:500 (Cell Signaling Technology) at 4°C. Then they were washed with 0.05% TBST 3 times for 10 minutes each wash. After washing, membranes were incubated with corresponding horseradish peroxidase–linked IgG in 0.05% TBST (1:7000) containing 5% NFDM for 60 minutes at room temperature. After a final washing, blots were developed by enzyme chemiluminescence (Bio-Rad), and immunoreactive proteins were visualized on film. The blots were stripped and reprobed with an anti–β-actin antibody (clone AC-15, MilliporeSigma). Densitometric analysis of the blots was done using ImageJ software as per standard protocol provided by the NIH.

ELISA for IL-1β, IL-6, CCL3, TNF-α, TIMP-1, MMP-9, and IL-4. Sandwich ELISA was done to determine the levels of IL-1β, IL-6, CCL3, TNF-α, TIMP-1, MMP-9, and IL-4. The cells were exposed to different treatments and their controls as per requirements for 16 hours. After brief centrifugation, cell culture supernatant samples were analyzed using human IL-1β, IL-6, CCL3, TNF-α, TIMP-1, MMP-9, and IL-4 ELISA kits (all from R&D Systems) according to the manufacturer's instructions.

Quantitative analysis was performed on a microplate reader (Thermo Fisher Scientific, accuSkan). A 4-parameter logistic curve was used to describe the data. For each experiment at least 2 replicates were used for analysis.

In vitro IL-1β cleavage assay. Pro–IL-1β, 31 kDa (purchased from OriGene Technologies, Inc.) (200 ng for each sample), was incubated with either 1 unit or 2 units of purified recombinant caspase-1, -2, -3, -4, -5, -6, -7, -8, -9, or -10 (all from BioVision, Inc.) for 2 hours alone in 20 μL of 2× reaction buffer (0.1 M HEPES buffer, pH 7.5 with 20% glycerol, 5 mM DTT, 0.5 mM EDTA) (containing 10 mM DTT) (BioVision, Inc.), at 37°C. A time-course experiment was also performed, where recombinant caspase-7 was incubated from 2 to 16 hours with pro–IL-1β. The resulting cleavage products were analyzed by Western blotting using anti–IL-1β antibody (R&D Systems).

Conditioned medium processing for Western blot. PBMCs of patients with AIED and controls were treated with 1 μg/mL LPS for 16 hours, cultured supernatant was gently lifted from cell culture plate, and to ensure there was no lysed cell contamination, conditioned supernatants were passed through a filter (MilliporeSigma) and centrifuged for an additional 30 minutes at 4°C to minimize any chance of contamination. Conditioned medium was then cooked with 4× sample buffer for 10 minutes and then analyzed by Western blot using IL-1β antibody (R&D Systems). Detection of actin (lack thereof) was performed to ensure there were no lysed cells within the supernatant.

Silver staining and high-resolution mass spectrometry (liquid chromatography tandem mass spectrometry). Pro–IL-1β, 31 kDa (purchased from OriGene Technologies, Inc.) (3500 ng), was incubated with purified recombinant caspase-7 (BioVision, Inc.) for 2 hours in 2× reaction buffer (BioVision, Inc.), at 37°C. The resulting cleavage product mix was loaded on 12% SDS-PAGE gels. The gel was silver stained using the mass spectrometry–compatible SilverQuest Silver Staining Kit (Invitrogen, Thermo Fisher Scientific). The 28-kDa band was visible on a silver-stained SDS-PAGE, and the band was excised for further analysis. Mass spectrometry analysis was performed at the Weill Cornell Medicine Meyer Cancer Center Proteomics and Metabolomics Core Facility (New York, New York, USA).

Statistics. Statistical analyses were performed with commercial software (GraphPad Prism version 5 and SAS Studio, SAS Institute Inc.). Data are expressed as the mean ± SEM. The Wilcoxon signed-rank test was performed for paired observations, to compare expression levels within groups, between 17-kDa and 28-kDa stimulation conditions.

Corrections for multiple testing were made using Bonferroni's adjustments. For each cytokine studied, a Bonferroni's adjustment was made for the 6 hypothesis tests carried out within that cytokine, such that any given comparison required $P < (0.05 / 6) = 0.0083$. No adjustment was made for testing multiple cytokine outcomes. For the pairwise comparison of 17-kDa and 28-kDa stimulation, a Bonferroni's adjustment was made for the 2 hypothesis tests carried out within a cytokine. No adjustment was made for testing of multiple cytokines or duplicate testing of ELISA and qPCR.

Study approval. The study protocol was approved by the Northwell Health System Institutional Review Board. Written consent was obtained prior to enrollment in the study. Inclusion and exclusion criteria were similar to those the AIED study group published previously (2). A total of 41 patients with AIED and 32 healthy controls were enrolled in this study; the average age of the patients with AIED was 51 with a 1.3:1 male-to-female ratio, and the average age of the control subjects was 48 with a male-to-female ratio of 1:1.9.

Author contributions

SP and AV designed the study. SP performed experiments and collected the data. SP and AV analyzed the data. SP and AV wrote the manuscript.

Acknowledgments

This study was supported by NIH grant R33DC011827 (AV) and Merrill & Phoebe Goodman Otology Research Center. We are grateful to Betty Diamond for her critical review of this manuscript. We would like to thank Martin Lesser and Karalyn Pappas for performing the statistical analysis.

Address correspondence to: Andrea Vambutas, Feinstein Institute for Medical Research, Donald and Barbara Zucker School of Medicine at Hofstra/Northwell, 350 Community Drive, Manhasset, New York 11030, USA. Phone: 718.470.7748; Email: avambuta@northwell.edu.

1. Vambutas A, Pathak S. AAO: Autoimmune and Autoinflammatory (Disease) in Otology: what is new in immune-mediated hearing loss. *Laryngoscope Investig Otolaryngol*. 2016;1(5):110–115.
2. Niparko JK, et al. Serial audiometry in a clinical trial of AIED treatment. *Otol Neurotol*. 2005;26(5):908–917.
3. Broughton SS, Meyerhoff WE, Cohen SB. Immune-mediated inner ear disease: 10-year experience. *Semin Arthritis Rheum*. 2004;34(2):544–548.
4. Harris JP, et al. Treatment of corticosteroid-responsive autoimmune inner ear disease with methotrexate: a randomized controlled trial. *JAMA*. 2003;290(14):1875–1883.
5. Cohen S, Shoup A, Weisman MH, Harris J. Etanercept treatment for autoimmune inner ear disease: results of a pilot placebo-controlled study. *Otol Neurotol*. 2005;26(5):903–907.
6. Solares CA, et al. Murine autoimmune hearing loss mediated by CD4+ T cells specific for inner ear peptides. *J Clin Invest*. 2004;113(8):1210–1217.
7. Satoh H, Firestein GS, Billings PB, Harris JP, Keithley EM. Proinflammatory cytokine expression in the endolymphatic sac during inner ear inflammation. *J Assoc Res Otolaryngol*. 2003;4(2):139–147.
8. Matteson EL, et al. Etanercept therapy for immune-mediated cochleovestibular disorders: a multi-center, open-label, pilot study. *Arthritis Rheum*. 2005;53(3):337–342.
9. Vambutas A, DeVoti J, Goldofsky E, Gordon M, Lesser M, Bonagura V. Alternate splicing of interleukin-1 receptor type II (IL1R2) in vitro correlates with clinical glucocorticoid responsiveness in patients with AIED. *PLoS ONE*. 2009;4(4):e5293.
10. Pathak S, Goldofsky E, Vivas EX, Bonagura VR, Vambutas A. IL-1β is overexpressed and aberrantly regulated in corticosteroid nonresponders with autoimmune inner ear disease. *J Immunol*. 2011;186(3):1870–1879.
11. Mandrup-Poulsen T, Pickersgill L, Donath MY. Blockade of interleukin 1 in type 1 diabetes mellitus. *Nat Rev Endocrinol*. 2010;6(3):158–166.
12. Arend WP. Cytokine imbalance in the pathogenesis of rheumatoid arthritis: the role of interleukin-1 receptor antagonist. *Semin Arthritis Rheum*. 2001;30(5 Suppl 2):1–6.
13. Luheshi NM, Rothwell NJ, Brough D. Dual functionality of interleukin-1 family cytokines: implications for antiinterleukin-1 therapy. *Br J Pharmacol*. 2009;157(8):1318–1329.
14. Ligumsky M, Simon PL, Karmeli F, Rachmilewitz D. Role of interleukin 1 in inflammatory bowel disease--enhanced production during active disease. *Gut*. 1990;31(6):686–689.
15. Gosselin D, Rivest S. Role of IL-1 and TNF in the brain: twenty years of progress on a Dr. Jekyll/Mr. Hyde duality of the innate immune system. *Brain Behav Immun*. 2007;21(3):281–289.
16. Hawkins PN, Lachmann HJ, McDermott MF. Interleukin-1-receptor antagonist in the Muckle-Wells syndrome. *N Engl J Med*. 2003;348(25):2583–2584.
17. Hull KM, Shoham N, Chae JJ, Aksentijevich I, Kastner DL. The expanding spectrum of systemic autoinflammatory disorders and their rheumatic manifestations. *Curr Opin Rheumatol*. 2003;15(1):61–69.
18. Gattorno M, Martini A. Beyond the NLRP3 inflammasome: autoinflammatory diseases reach adolescence. *Arthritis Rheum*. 2013;65(5):1137–1147.
19. Agostini L, Martinon F, Burns K, McDermott MF, Hawkins PN, Tschopp J. NALP3 forms an IL-1beta-processing inflammasome with increased activity in Muckle-Wells autoinflammatory disorder. *Immunity*. 2004;20(3):319–325.
20. Stojanov S, Kastner DL. Familial autoinflammatory diseases: genetics, pathogenesis and treatment. *Curr Opin Rheumatol*. 2005;17(5):586–599.
21. Church LD, Cook GP, McDermott MF. Primer: inflammasomes and interleukin 1beta in inflammatory disorders. *Nat Clin Pract Rheumatol*. 2008;4(1):34–42.
22. Gattorno M, et al. Pattern of interleukin-1beta secretion in response to lipopolysaccharide and ATP before and after interleukin-1 blockade in patients with CIAS1 mutations. *Arthritis Rheum*. 2007;56(9):3138–3148.
23. Vambutas A, et al. Early efficacy trial of anakinra in corticosteroid-resistant autoimmune inner ear disease. *J Clin Invest*. 2014;124(9):4115–4122.
24. Dinarello CA. Immunological and inflammatory functions of the interleukin-1 family. *Annu Rev Immunol*. 2009;27:519–550.
25. Dinarello CA. Biologic basis for interleukin-1 in disease. *Blood*. 1996;87(6):2095–2147.
26. Sasaki H, et al. Induction of heat shock protein 47 synthesis by TGF-beta and IL-1 beta via enhancement of the heat shock element binding activity of heat shock transcription factor 1. *J Immunol*. 2002;168(10):5178–5183.
27. Cheng CY, Kuo CT, Lin CC, Hsieh HL, Yang CM. IL-1beta induces expression of matrix metalloproteinase-9 and cell migration via a c-Src-dependent, growth factor receptor transactivation in A549 cells. *Br J Pharmacol*. 2010;160(7):1595–1610.
28. Siwik DA, Colucci WS. Regulation of matrix metalloproteinases by cytokines and reactive oxygen/nitrogen species in the myocardium. *Heart Fail Rev*. 2004;9(1):43–51.
29. Wu CY, Hsieh HL, Sun CC, Yang CM. IL-1beta induces MMP-9 expression via a Ca2+-dependent CaMKII/JNK/c-JUN cascade in rat brain astrocytes. *Glia*. 2009;57(16):1775–1789.
30. Agrawal S, et al. Dystroglycan is selectively cleaved at the parenchymal basement membrane at sites of leukocyte extravasation in experimental autoimmune encephalomyelitis. *J Exp Med*. 2006;203(4):1007–1019.
31. Han R, Smith TJ. Induction by IL-1 beta of tissue inhibitor of metalloproteinase-1 in human orbital fibroblasts: modulation of gene promoter activity by IL-4 and IFN-gamma. *J Immunol*. 2005;174(5):3072–3079.
32. Eisner L, Vambutas A, Pathak S. The balance of tissue inhibitor of metalloproteinase-1 and matrix metalloproteinase-9 in the autoimmune inner ear disease patients. *J Interferon Cytokine Res*. 2017;37(8):354–361.
33. Guo CJ, et al. Interleukin-1beta stimulates macrophage inflammatory protein-1alpha and -1beta expression in human neuronal cells (NT2-N). *J Neurochem*. 2003;84(5):997–1005.
34. Wang J, et al. Tumor necrosis factor α- and interleukin-1β-dependent induction of CCL3 expression by nucleus pulposus cells promotes macrophage migration through CCR1. *Arthritis Rheum*. 2013;65(3):832–842.
35. Thornberry NA, et al. A novel heterodimeric cysteine protease is required for interleukin-1 beta processing in monocytes. *Nature*. 1992;356(6372):768–774.
36. Arend WP, Palmer G, Gabay C. IL-1, IL-18, and IL-33 families of cytokines. *Immunol Rev*. 2008;223:20–38.

37. Black RA, Kronheim SR, Sleath PR. Activation of interleukin-1 beta by a co-induced protease. *FEBS Lett*. 1989;247(2):386–390.
38. Kostura MJ, et al. Identification of a monocyte specific pre-interleukin 1 beta convertase activity. *Proc Natl Acad Sci USA*. 1989;86(14):5227–5231.
39. Sleath PR, Hendrickson RC, Kronheim SR, March CJ, Black RA. Substrate specificity of the protease that processes human interleukin-1 beta. *J Biol Chem*. 1990;265(24):14526–14528.
40. Kuida K, et al. Altered cytokine export and apoptosis in mice deficient in interleukin-1 beta converting enzyme. *Science*. 1995;267(5206):2000–2003.
41. Limjuco G, Galuska S, Chin J, Cameron P, Boger J, Schmidt JA. Antibodies of predetermined specificity to the major charged species of human interleukin 1. *Proc Natl Acad Sci USA*. 1986;83(11):3972–3976.
42. Cameron P, Limjuco G, Rodkey J, Bennett C, Schmidt JA. Amino acid sequence analysis of human interleukin 1 (IL-1). Evidence for biochemically distinct forms of IL-1. *J Exp Med*. 1985;162(3):790–801.
43. March CJ, et al. Cloning, sequence and expression of two distinct human interleukin-1 complementary DNAs. *Nature*. 1985;315(6021):641–647.
44. Auron PE, et al. Studies on the molecular nature of human interleukin 1. *J Immunol*. 1987;138(5):1447–1456.
45. Howard AD, et al. IL-1-converting enzyme requires aspartic acid residues for processing of the IL-1 beta precursor at two distinct sites and does not cleave 31-kDa IL-1 alpha. *J Immunol*. 1991;147(9):2964–2969.
46. Puren AJ, Fantuzzi G, Dinarello CA. Gene expression, synthesis, and secretion of interleukin 18 and interleukin 1beta are differentially regulated in human blood mononuclear cells and mouse spleen cells. *Proc Natl Acad Sci USA*. 1999;96(5):2256–2261.
47. Maelfait J, et al. Stimulation of Toll-like receptor 3 and 4 induces interleukin-1beta maturation by caspase-8. *J Exp Med*. 2008;205(9):1967–1973.
48. Schönbeck U, Mach F, Libby P. Generation of biologically active IL-1 beta by matrix metalloproteinases: a novel caspase-1-independent pathway of IL-1 beta processing. *J Immunol*. 1998;161(7):3340–3346.
49. Davaro F, et al. 3-Hydroxyl-3-methylglutaryl coenzyme A (HMG-CoA) reductase inhibitor (statin)-induced 28-kDa interleukin-1β interferes with mature IL-1β signaling. *J Biol Chem*. 2014;289(23):16214–16222.
50. Schumann RR, et al. Lipopolysaccharide activates caspase-1 (interleukin-1-converting enzyme) in cultured monocytic and endothelial cells. *Blood*. 1998;91(2):577–584.
51. Towne JE, et al. Interleukin-36 (IL-36) ligands require processing for full agonist (IL-36α, IL-36β, and IL-36γ) or antagonist (IL-36Ra) activity. *J Biol Chem*. 2011;286(49):42594–42602.
52. Clancy DM, Henry CM, Davidovich PB, Sullivan GP, Belotcerkovskaya E, Martin SJ. Production of biologically active IL-36 family cytokines through insertion of N-terminal caspase cleavage motifs. *FEBS Open Bio*. 2016;6(4):338–348.
53. Walsh JG, Cullen SP, Sheridan C, Lüthi AU, Gerner C, Martin SJ. Executioner caspase-3 and caspase-7 are functionally distinct proteases. *Proc Natl Acad Sci USA*. 2008;105(35):12815–12819.
54. Erener S, et al. Inflammasome-activated caspase 7 cleaves PARP1 to enhance the expression of a subset of NF-κB target genes. *Mol Cell*. 2012;46(2):200–211.
55. Lamkanfi M, et al. Caspase-7 deficiency protects from endotoxin-induced lymphocyte apoptosis and improves survival. *Blood*. 2009;113(12):2742–2745.
56. Hoffer ME, Allen K, Kopke RD, Weisskopf P, Gottshall K, Wester D. Transtympanic versus sustained-release administration of gentamicin: kinetics, morphology, and function. *Laryngoscope*. 2001;111(8):1343–1357.
57. Burguillos MA, et al. Caspase signalling controls microglia activation and neurotoxicity. *Nature*. 2011;472(7343):319–324.
58. Bhave SA, Oesterle EC, Coltrera MD. Macrophage and microglia-like cells in the avian inner ear. *J Comp Neurol*. 1998;398(2):241–256.
59. Hirose K, Discolo CM, Keasler JR, Ransohoff R. Mononuclear phagocytes migrate into the murine cochlea after acoustic trauma. *J Comp Neurol*. 2005;489(2):180–194.
60. O'Malley JT, Nadol JB, McKenna MJ. Anti CD163+, Iba1+, and CD68+ cells in the adult human inner ear: normal distribution of an unappreciated class of macrophages/microglia and implications for inflammatory otopathology in humans. *Otol Neurotol*. 2016;37(1):99–108.
61. Thornberry NA, Lazebnik Y. Caspases: enemies within. *Science*. 1998;281(5381):1312–1316.